Advances in Nano Research, *Vol. 8, No. 4 (2020) 265-276*
DOI: https://doi.org/10.12989/anr.2020.8.4.265

Investigating vibrational behavior of graphene sheets under linearly varying in-plane bending load based on the nonlocal strain gradient theory

Ali Shariati [1,2a], Mohammad Reza Barati [3], Farzad Ebrahimi[*3], Abhinav Singhal [4] and Ali Toghroli[**5]

[1] *Division of Computational Mathematics and Engineering, Institute for Computational Science, Ton Duc Thang University, Ho Chi Minh City, 758307, Vietnam*
[2] *Faculty of Civil Engineering, Ton Duc Thang University, Ho Chi Minh City, 758307, Vietnam*
[3] *Department of Mechanical Engineering, Faculty of Engineering, Imam Khomeini International University, Qazvin, Iran*
[4] *Department of Mathematics, Madanapalle Institute of Technology and Science, Madanapalle, Andhra Pradesh, 517325, India*
[5] *Institute of Research and Development, Duy Tan University, Da Nang 550000, Vietnam*

(*Received May 25, 2019, Revised October 28, 2019, Accepted November 14, 2019*)

Abstract. A study that primarily focuses on nonlocal strain gradient plate model for the sole purpose of vibration examination, for graphene sheets under linearly variable in-plane mechanical loads. To study a better or more precise examination on graphene sheets, a new advance model was conducted which carries two scale parameters that happen to be related to the nonlocal as well as the strain gradient influences. Through the usage of two-variable shear deformation plate approach, that does not require the inclusion of shear correction factors, the graphene sheet is designed. Based on Hamilton's principle, fundamental expressions in regard to a nonlocal strain gradient graphene sheet on elastic half-space is originated. A Galerkin's technique is applied to resolve the fundamental expressions for distinct boundary conditions. Influence of distinct factors which can be in-plane loading, length scale parameter, load factor, elastic foundation, boundary conditions, and nonlocal parameter on vibration properties of the graphene sheets then undergo investigation.

Keywords: graphene sheets; free vibration; in-plane bending; nonlocal strain gradient; refined plate theory

1. Introduction

Graphene is one of the special material, which has enough applications in engineering due to their attractive properties because of having atomic crystal of two-dimension with remarkable mechanical and electronic properties. One of the highly used material in the field of nanotechnology is graphene. Graphene is formed out of carbon which has chemically stable two-dimensional one atom thick sheet. This feature from carbon allows graphene to be one of the strongest and thinnest material available.

In research, now a day's graphene is too applicable. Therefore, enormous number of nanostructures relying on carbons viz., carbon nanobeams, nanotubes, nanoplates, etc. called deformed carbon sheets (Ebrahimi and Salari 2015). To know the characteristics of nanomaterial, there is an only best-known way is the examination of graphene sheets, only for those nanostructures, which are relying on graphene material. Large amount of literature is available which carries the theory of examination of scale-free plates. But, there is a shortcoming in a theory to examine on scale free plates, which is they did not analyze on nanostructures of small size. Due to that, nonlocal theory of elasticity by Eringen (Eringen and Edelen 1972, Eringen 1983) is created and useful for nanostructure of small size. Moreover, elasticity theory of nonlocal is broadly applicable in the nanoscale structure for the examination of their mechanical characteristics (Ebrahimi and Barati 2016a-f).

The nonlocal impact over buckling behavior of graphene solitary-plate subjected loading (uniform in-plane) is investigated by Pradhan and Murmu (2009). Some studies related to motions in the form of vibration had been explored by Pradhan and Kumar (2011) in orthotropic sheets assimilated to nonlocal influence. Application with importance of Levy type technique of stability along with trembling examination of nanosize thin plates that happen to experience nonlocal influence that is analyzed by Aksencer and Aydogdu (2011). The examination of shear buckling of an orthotropic graphene thin sheets resting on an elastic half-space which experiences the influence of thermal loading, has been inspected carefully by Mohammadi *et al.* (2014). Afterwards, Mohammadi *et al.* (2013) set-up an investigation to discover the behavior of nonlocal vibrations of graphene sheets (circular shape) which are influenced by in-plane loading. Ansari *et al.* (2011) beautifully examined the responses of vibrations of embedded multifold-layered sheets of graphene material, which accounts for varied boundary conditions. Moreover, some renowned work has been done on graphene sheets, i.e. vibrational study of mass sensor, static capacity of nonlocal thin sheets facing non-uniform edge-load, buckling

*Corresponding author, Ph.D.,
E-mail: febrahimy@eng.ikiu.ac.ir
**Co-corresponding author, Ph.D. Candidate,
E-mail: alitoghroli@duytan.edu.vn
[a] Ph.D. Candidate, E-mail: alishariati@tdtu.edu.vn

ISSN: 2287-237X (Print), 2287-2388 (Online)

behavior (biaxial) of graphene single layer sheet that relies on the nonlocal elasticity theory by Shen *et al*. (2012), Farajpour *et al*. (2012) and Ansari and Sahmani (2013) respectively. Sobhy (2014) completed a study in regard to vibrational and static bending nature of graphene sheets (single layer) based on Winkler-Pasternak foundation which relies on a 2-variable higher order shear deformation theory. Afterwards, stability size-dependent examination of nanoscale orthotropic plates following the theory of nonlocal two-variable refined plates has been carried out by Narendar and Gopalakrishnan (2012). Murmu *et al*. (2013) precisely examined effects of unidirectional magnetic fields on vibrational characteristics of graphene sheets stick on elastic half-space. Moreover, Bessaim *et al*. (2015), Hashemi *et al*. (2015) and Ebrahimi and Shafiei (2016) studied the nonlocal quasi-3D trigonometric plate model, free vibrational nature of bi-viscielastic graphene thin sheets coupled with visco-Pasternak medium as well as effect of initial stress in graphene sheets by integrating Reddy's higher order shear deformation theory.

Throughout the course of the investigation that has been described above, it is clear that all the literature is carried out by using the elasticity theory of nonlocal in view of small scale effects. Furthermore, the nonlocal elasticity concept shows critical restrictions when nanostructures characteristics are going to be predicted. Keeping in view of these shortcomings in the theory of nonlocal elasticity, some researchers discovered how the nonlocal strain gradient theory may in fact assist to overcome or control the shortcomings viz., Lam *et al*. (2003), Tian *et al*. (2018), Stelson (2018), Henderson *et al*. (2018).

Most recently, Ebrahimi and Barati (2016a-m) have also advanced the nonlocal strain gradient theory further, with the means of examining thin Nano plates of distinct plates. Therefore, it is significant to incorporate strain gradient and nonlocal influence in examination of graphene sheets priory as it can affect the examination of thin Nano plates of distinct plates.

Relying on the new advanced nonlocal strain gradient theory, the vibrational characteristics of single-layered graphene thin sheets facing bending in-plane loadings stick on elastic material medium is sensibly investigated by theory i.e., refined two-variable plate theory. According to Hamiltons's principle, fundamental expressions of the nonlocal strain gradient graphene sheet on elastic half-space are originated. A Galerkin's technique is applied in order to resolve fundamental expressions for the distinct boundary conditions. Influence of distinct factors which can be in-plane loading, length scale parameter, load factor, elastic foundation, boundary conditions, as well as nonlocal parameter on vibration properties of a graphene sheets are investigated. Self-consolidating concrete is a kind of concrete which fluidity and workability parameters have to be enhanced in it (Ebrahimi and Salari 2015), hence using graphene sprayed on the surface of aggregated could improve the SCC fluidity properties and further elevate how the material operates or functions. Furthermore, using graphene processed materials could be applied in numerous applications during construction, where the nano-scale properties of the graphene sheets or sprays are able to mitigate some micro-structural deficiencies as steel micro crack and stain in cold-formed steel uprights (Erigen and Edelen 1972, Eringen 1983, Ebrahimi and Barati 2016a-e) or cover the flexural and compressive strength loss during cyclic and motonic loading scenarios. It is important to note that there are different available techniques for data validations and predictions such as employing artificial neural networks (Ebrahimi and Barati 2016f, Pradhan and Murmu 2009, Pradhan and Kumar 2011, Aksencer and Aydogdu 2011, Mohammadi *et al*. 2013, 2014), Finite element method (Erigen and Edelen 1972, Eringen 1983, Ansari *et al*. 2011), Finite strip method (Shen *et al*. 2012, Farajpour *et al*. 2012, Ansari and Sahmani 2013). Finite element method which is generally carried out by FE programs as ABAQUS and ANSYS performed which are known for their reliable technique for empirical data validation and response analysis and prediction.

2. Governing equations

The following displacement field are given by using the higher-order advanced plate theory

$$u_1(x,y,z) = -z\frac{\partial w_b}{\partial x} - f(z)\frac{\partial w_s}{\partial x} \tag{1}$$

$$u_2(x,y,z) = -z\frac{\partial w_b}{\partial y} - f(z)\frac{\partial w_s}{\partial y} \tag{2}$$

$$u_3(x,y,z) = w_b(x,y) + w_s(x,y) \tag{3}$$

Now, in the above equations there is a trigonometric function, which as

$$f(z) = z - \frac{h}{\pi} sin\left(\frac{\pi z}{h}\right) \tag{4}$$

where, w_b represents the bending transverse displacement and subsequently w_s, represents the shear transverse displacement. Now, strains (nonzero) of considered thin plate model is able to be expressed through

$$\begin{Bmatrix}\varepsilon_x\\ \varepsilon_y\\ \gamma_{xy}\end{Bmatrix} = +z\begin{Bmatrix}\kappa_x^b\\ \kappa_y^b\\ \kappa_{xy}^b\end{Bmatrix} + f(z)\begin{Bmatrix}\kappa_x^s\\ \kappa_y^s\\ \kappa_{xy}^s\end{Bmatrix}, \quad \begin{Bmatrix}\gamma_{yz}\\ \gamma_{xz}\end{Bmatrix} = g(z)\begin{Bmatrix}\gamma_{yz}^s\\ \gamma_{xz}^s\end{Bmatrix} \tag{5}$$

Where, the assuming function $g(z) = 1 - df/dz$, and

$$\begin{Bmatrix}\kappa_x^b\\ \kappa_y^b\\ \kappa_{xy}^b\end{Bmatrix} = \begin{Bmatrix}-\frac{\partial^2 w_b}{\partial x^2}\\ -\frac{\partial^2 w_b}{\partial y^2}\\ -2\frac{\partial^2 w_b}{\partial x \partial y}\end{Bmatrix}, \quad \begin{Bmatrix}\kappa_x^s\\ \kappa_y^s\\ \kappa_{xy}^s\end{Bmatrix} = \begin{Bmatrix}-\frac{\partial^2 w_s}{\partial x^2}\\ -\frac{\partial^2 w_s}{\partial y^2}\\ -2\frac{\partial^2 w_s}{\partial x \partial y}\end{Bmatrix}, \quad \begin{Bmatrix}\gamma_{yz}^s\\ \gamma_{xz}^s\end{Bmatrix} = \begin{Bmatrix}\frac{\partial w_s}{\partial y}\\ \frac{\partial w_s}{\partial x}\end{Bmatrix} \tag{6}$$

Now, from the Hamilton's principle we have

$$\int_0^t \delta(U - T + V)dt = 0 \tag{7}$$

Where, U symbolizes the strain energy in the equation, T then represents the kinetic energy of the structure and meanwhile V symbolizes the work done, that is carried out by the external loads. Now, it is possible to express the variation of strain energy by

$$\begin{aligned}\delta U &= \int_v \sigma_{ij}\delta\varepsilon_{ij}dV \\ &= \int_v (\sigma_x\delta\varepsilon_x + \sigma_y\delta\varepsilon_y + \sigma_{xy}\delta\gamma_{xy} + \sigma_{yz}\delta\gamma_{yz} \\ &+\sigma_{xz}\delta\gamma_{xz})dV\end{aligned} \tag{8}$$

Introducing Eqs. (5)-(6) into Eq. (8), which consequently produces

$$\begin{aligned}\delta U = \int_0^b\int_0^a \Big[&-M_x^b\frac{\partial^2\delta w_b}{\partial x^2} - M_x^s\frac{\partial^2\delta w_s}{\partial x^2} - M_y^b\frac{\partial^2\delta w_b}{\partial y^2} \\ &-M_y^s\frac{\partial^2\delta w_s}{\partial y^2} - 2M_{xy}^b\frac{\partial^2\delta w_b}{\partial x\partial y} - 2M_{xy}^s\frac{\partial^2\delta w_s}{\partial x\partial y} \\ &+Q_{yz}\frac{\partial\delta w_s}{\partial y} + Q_{xz}\frac{\partial\delta w_s}{\partial x}\Big]dxdy\end{aligned} \tag{9}$$

In Eq. (9), the *M* is given as

$$\begin{aligned}\left(M_i^b, M_i^s\right) &= \int_{-\frac{h}{2}}^{\frac{h}{2}}(z,f)\sigma_i\,dz, \qquad i = (x,y,xy) \\ Q_i &= \int_{-h/2}^{h/2} g\sigma_i\,dz, \qquad i = (xz,yz)\end{aligned} \tag{10}$$

The work done variation after applying all the loads is expressed through

$$\begin{aligned}\delta V = \int_0^b\int_0^a (&N_x^0\frac{\partial(w_b+w_s)}{\partial x}\frac{\partial\delta(w_b+w_s)}{\partial x} \\ &+N_y^0\frac{\partial(w_b+w_s)}{\partial y}\frac{\partial\delta(w_b+w_s)}{\partial y} \\ &+2\delta N_{xy}^0\frac{\partial(w_b+w_s)}{\partial x}\frac{\partial(w_b+w_s)}{\partial y} \\ &-k_w\delta(w_b+w_s) + k_p\delta(w_b+w_s))dxdy\end{aligned} \tag{11a}$$

Here, N_x^0, N_y^0, N_{xy}^0 represents the in-plane applied loads, also, K_w & K_p symbolizes the Winkler & Pasternak constants.

Essentially, we need to take into account a few assumptions where graphene thin sheet when undergoing the linearly varying load (in-plane) while loading is zero $N_{xy}^0 = 0$

$$N_x^0 = N(1 - \xi\frac{y}{b}), \qquad N_y^0 = \eta N(1 - \xi\frac{x}{a}) \tag{11b}$$

In above Eq. (11b), ξ symbolizes the in-plane bending load factor.

Now, kinetic energy variation is given as

$$\begin{aligned}\delta K = \int_0^b\int_0^a \Big[&I_0\left(\frac{\partial(w_b+w_s)}{\partial t}\frac{\partial\delta(w_b+w_s)}{\partial t}\right) \\ &+I_2\left(\frac{\partial w_b}{\partial x\partial t}\frac{\partial\delta w_b}{\partial x\partial t} + \frac{\partial w_b}{\partial y\partial t}\frac{\partial\delta w_b}{\partial y\partial t}\right) \\ &+K_2\left(\frac{\partial w_s}{\partial x\partial t}\frac{\partial\delta w_s}{\partial x\partial t} + \frac{\partial w_s}{\partial y\partial t}\frac{\partial\delta w_s}{\partial y\partial t}\right) \\ &+J_2\left(\frac{\partial w_b}{\partial x\partial t}\frac{\partial\delta w_s}{\partial x\partial t} + \frac{\partial w_s}{\partial x\partial t}\frac{\partial\delta w_b}{\partial x\partial t} + \frac{\partial w_b}{\partial y\partial t}\frac{\partial\delta w_s}{\partial y\partial t}\right. \\ &\left.+\frac{\partial w_s}{\partial y\partial t}\frac{\partial\delta w_b}{\partial y\partial t}\right)\Big]dxdy\end{aligned} \tag{12}$$

Where

$$\left(I_0\ , I_2\ , J_2\ , K_2\ \right) = \int_{-h/2}^{h/2}(1, z^2, zf, f^2)\rho dz \tag{13}$$

Through introducing the Eqs. (9)-(12) in Eq. (7) along with collecting coefficients of δw_b & δw_s as well as putting them equals to zero as by the necessary condition, then we reached upto the following equations

$$\begin{aligned}&\frac{\partial^2 M_x^b}{\partial x^2} + 2\frac{\partial^2 M_{xy}^b}{\partial x\partial y} + \frac{\partial^2 M_y^b}{\partial y^2} \\ &-N_x^0(y)\frac{\partial^2(w_b+w_s)}{\partial x^2} - N_y^0(x)\frac{\partial^2(w_b+w_s)}{\partial y^2} \\ &+k_p\left[\frac{\partial^2(w_b+w_s)}{\partial x^2} + \frac{\partial^2(w_b+w_s)}{\partial y^2}\right] - k_w(w_b+w_s) \\ &= I_0\frac{\partial^2(w_b+w_s)}{\partial t^2} - I_2\nabla^2\left(\frac{\partial^2 w_b}{\partial t^2}\right) - J_2\nabla^2\left(\frac{\partial^2 w_s}{\partial t^2}\right)\end{aligned} \tag{14}$$

$$\begin{aligned}&\frac{\partial^2 M_x^s}{\partial x^2} + 2\frac{\partial^2 M_{xy}^s}{\partial x\partial y} + \frac{\partial^2 M_y^s}{\partial y^2} + \frac{\partial Q_{xz}}{\partial x} + \frac{\partial Q_{yz}}{\partial y} \\ &-N_x^0(y)\frac{\partial^2(w_b+w_s)}{\partial x^2} - N_y^0(x)\frac{\partial^2(w_b+w_s)}{\partial y^2} \\ &+k_p\left[\frac{\partial^2(w_b+w_s)}{\partial x^2} + \frac{\partial^2(w_b+w_s)}{\partial y^2}\right] - k_w(w_b+w_s) \\ &= I_0\frac{\partial^2(w_b+w_s)}{\partial t^2} - J_2\nabla^2\left(\frac{\partial^2 w_b}{\partial t^2}\right) - K_2\nabla^2\left(\frac{\partial^2 w_s}{\partial t^2}\right)\end{aligned} \tag{15}$$

Hence, the Eq. (15) is derived.

2.1 An analysis of the nonlocal strain gradient nanoplate structure

A recently advanced nonlocal strain gradient theory (Ebrahimi and Barati 2016a) happens to include a factor that has been developed specifically for strain gradients and nonlocal stress field effects with the help of two scale parameters. The newly considered theory delineate the stress field as

$$\sigma_{ij} = \sigma_{ij}^{(0)} - \frac{d\sigma_{ij}^{(1)}}{dx} \tag{16}$$

Where, the stresses $\sigma_{xx}^{(0)}$ & $\sigma_{xx}^{(1)}$ in relation with strain ε_{xx} & strain gradient $\varepsilon_{xx,x}$, correspondingly as

$$\sigma_{ij}^{(0)} = \int_0^L C_{ijkl}\,\alpha_0(x,x',e_0a)\varepsilon_{kl}'(x')dx' \tag{17a}$$

$$\sigma_{ij}^{(1)} = l^2 \int_0^L C_{ijkl}\, \alpha_1(x, x', e_1 a) \varepsilon'_{kl,x}(x') dx' \tag{17b}$$

Where, C_{ijkl} represents two elastic coefficients, namely, e_0a & e_1a holds the nonlocal influence, while l represents the strain gradient influence. In addition to that, the functions, which are nonlocal, i.e., $\alpha_0(x, x', e_0 a)$ &$\alpha_1(x, x', e_1 a)$ assures that conditions that are established from (Eringen 1983) demonstrate all the necessary or essential correlations for the nonlocal strain gradient theory subsequently through

$$\begin{aligned} &[1-(e_1a)^2\nabla^2][1-(e_0a)^2\nabla^2]\sigma_{ij} \\ &= C_{ijkl}[1-(e_1a)^2\nabla^2]\varepsilon_{kl} \\ &-C_{ijkl}l^2[1-(e_0a)^2\nabla^2]\nabla^2\varepsilon_{kl} \end{aligned} \tag{18}$$

Whereby, ∇^2 happens to be a representation of the Laplacian operator.

Taking into an account $e_1 = e_0 = e$, the essential correlation in Eq. (22a) set off

$$[1-(ea)^2\nabla^2]\sigma_{ij} = C_{ijkl}[1-l^2\nabla^2]\varepsilon_{kl} \tag{19}$$

At last, the essential correlation of the nonlocal strain gradient theory may be demonstrated with

$$\begin{aligned} &(1-\mu\nabla^2)\begin{Bmatrix}\sigma_x\\ \sigma_y\\ \sigma_{xy}\\ \sigma_{yz}\\ \sigma_{xz}\end{Bmatrix} \\ &= (1-\lambda\nabla^2)\begin{pmatrix} Q_{11} & Q_{12} & 0 & 0 & 0\\ Q_{12} & Q_{22} & 0 & 0 & 0\\ 0 & 0 & Q_{66} & 0 & 0\\ 0 & 0 & 0 & Q_{44} & 0\\ 0 & 0 & 0 & 0 & Q_{55}\end{pmatrix}\begin{Bmatrix}\varepsilon_x\\ \varepsilon_y\\ \gamma_{xy}\\ \gamma_{yz}\\ \gamma_{xz}\end{Bmatrix} \end{aligned} \tag{20}$$

where

$$\begin{aligned} &Q_{11} = Q_{22} = \frac{E}{1-\upsilon^2}, \quad Q_{12} = \upsilon Q_{11}, \\ &Q_{44} = Q_{55} = Q_{66} = \frac{E}{2(1+\upsilon)} \end{aligned} \tag{21}$$

where $\mu = (ea)^2$ & $\lambda = l^2$. Introducing Eq. (10) in Eq. (23) yields

$$\begin{aligned} &(1-\mu\nabla^2)\begin{Bmatrix}M_x^b\\ M_y^b\\ M_{xy}^b\end{Bmatrix} \\ &= (1-\lambda\nabla^2)\left[\begin{pmatrix} D_{11} & D_{12} & 0\\ D_{12} & D_{22} & 0\\ 0 & 0 & D_{66}\end{pmatrix}\begin{Bmatrix} -\dfrac{\partial^2 w_b}{\partial x^2}\\ -\dfrac{\partial^2 w_b}{\partial y^2}\\ -2\dfrac{\partial^2 w_b}{\partial x \partial y}\end{Bmatrix}\right. \\ &\left.+\begin{pmatrix} D_{11}^s & D_{12}^s & 0\\ D_{12}^s & D_{22}^s & 0\\ 0 & 0 & D_{66}^s\end{pmatrix}\begin{Bmatrix} -\dfrac{\partial^2 w_s}{\partial x^2}\\ -\dfrac{\partial^2 w_s}{\partial y^2}\\ -2\dfrac{\partial^2 w_s}{\partial x \partial y}\end{Bmatrix}\right] \end{aligned} \tag{22}$$

$$\begin{aligned} &(1-\mu\nabla^2)\begin{Bmatrix}M_x^s\\ M_y^s\\ M_{xy}^s\end{Bmatrix} \\ &= (1-\lambda\nabla^2)\left[\begin{pmatrix} D_{11}^s & D_{12}^s & 0\\ D_{12}^s & D_{22}^s & 0\\ 0 & 0 & D_{66}^s\end{pmatrix}\begin{Bmatrix} -\dfrac{\partial^2 w_b}{\partial x^2}\\ -\dfrac{\partial^2 w_b}{\partial y^2}\\ -2\dfrac{\partial^2 w_b}{\partial x \partial y}\end{Bmatrix}\right. \\ &\left.+\begin{pmatrix} H_{11}^s & H_{12}^s & 0\\ H_{12}^s & H_{22}^s & 0\\ 0 & 0 & H_{66}^s\end{pmatrix}\begin{Bmatrix} -\dfrac{\partial^2 w_s}{\partial x^2}\\ -\dfrac{\partial^2 w_s}{\partial y^2}\\ -2\dfrac{\partial^2 w_s}{\partial x \partial y}\end{Bmatrix}\right] \end{aligned} \tag{23}$$

$$(1-\mu\nabla^2)\begin{Bmatrix}Q_x\\ Q_y\end{Bmatrix} = (1-\lambda\nabla^2)\left[\begin{pmatrix} A_{44}^s & 0\\ 0 & A_{55}^s\end{pmatrix}\begin{Bmatrix}\dfrac{\partial w_s}{\partial x}\\ \dfrac{\partial w_s}{\partial y}\end{Bmatrix}\right] \tag{24}$$

Where, circular thin slice rigidities are as follows

.

$$\begin{Bmatrix} D_{11}, D_{11}^s, H_{11}^s\\ D_{12}, D_{12}^s, H_{12}^s\\ D_{66}, D_{66}^s, H_{66}^s\end{Bmatrix} = \int_{-h/2}^{h/2} Q_{11}(z^2, zf, f^2)\begin{Bmatrix}1\\ \nu\\ \dfrac{1-\nu}{2}\end{Bmatrix} dz \tag{25}$$

$$A_{44}^s = A_{55}^s = \int_{-h/2}^{h/2} g^2 \frac{E}{2(1+\nu)} dz \tag{26}$$

The fundamental expressions of nonlocal strain gradient graphene thin sheet in words of the displacement have been achieved through introducing Eqs. (25)-(27), into Eqs. (14)-(15) as shown further below

$$\begin{aligned} &-D_{11}\left[\frac{\partial^4 w_b}{\partial x^4} - \lambda\left(\frac{\partial^6 w_b}{\partial x^6} + \frac{\partial^6 w_b}{\partial x^4 \partial y^2}\right)\right] \\ &-2(D_{12}+2D_{66})\left[\frac{\partial^4 w_b}{\partial x^2 \partial y^2} - \lambda\left(\frac{\partial^6 w_b}{\partial x^4 \partial y^2} + \frac{\partial^6 w_b}{\partial x^2 \partial y^4}\right)\right] \\ &-D_{22}[\frac{\partial^4 w_b}{\partial y^4} - \lambda(\frac{\partial^6 w_b}{\partial y^6} + \frac{\partial^6 w_b}{\partial y^4 \partial x^2})] - D_{11}^s[\frac{\partial^4 w_s}{\partial x^4} \\ &-\lambda(\frac{\partial^6 w_s}{\partial x^6} + \frac{\partial^6 w_s}{\partial x^4 \partial y^2})] - 2(D_{12}^s + 2D_{66}^s)[\frac{\partial^4 w_s}{\partial x^2 \partial y^2} \\ &-\lambda(\frac{\partial^6 w_s}{\partial x^4 \partial y^2} + \frac{\partial^6 w_s}{\partial x^2 \partial y^4})] \\ &-D_{22}^s[\frac{\partial^4 w_s}{\partial y^4} - \lambda(\frac{\partial^6 w_s}{\partial y^6} + \frac{\partial^6 w_s}{\partial y^4 \partial x^2})] - I_0[\frac{\partial^2 (w_b + w_s)}{\partial t^2} \end{aligned} \tag{27}$$

$$
\begin{aligned}
&-\mu\left(\frac{\partial^4(w_b+w_s)}{\partial t^2\partial x^2}+\frac{\partial^4(w_b+w_s)}{\partial t^2\partial y^2}\right)]+I_2[\frac{\partial^4 w_b}{\partial x^2\partial t^2}\\
&+\frac{\partial^4 w_b}{\partial y^2\partial t^2}-\mu\left(\frac{\partial^6 w_b}{\partial t^2\partial x^4}+2\frac{\partial^6 w_b}{\partial t^2\partial x^2\partial y^2}+\frac{\partial^6 w_b}{\partial t^2\partial y^4}\right)]\\
&+J_2[\frac{\partial^4 w_s}{\partial x^2\partial t^2}+\frac{\partial^4 w_s}{\partial y^2\partial t^2}\\
&-\mu\left(\frac{\partial^6 w_s}{\partial t^2\partial x^4}+2\frac{\partial^6 w_s}{\partial t^2\partial x^2\partial y^2}+\frac{\partial^6 w_s}{\partial t^2\partial y^4}\right)]\\
&-N_x^0(y)\left[1-\mu\left(\frac{\partial^2}{\partial x^2}+\frac{\partial^2}{\partial y^2}\right)\right]\frac{\partial^2(w_b+w_s)}{\partial x^2}\\
&-N_y^0(x)\left[1-\mu\left(\frac{\partial^2}{\partial x^2}+\frac{\partial^2}{\partial y^2}\right)\right]\frac{\partial^2(w_b+w_s)}{\partial y^2}\\
&+k_p[1-\mu\left(\frac{\partial^2}{\partial x^2}+\frac{\partial^2}{\partial y^2}\right)][\frac{\partial^2(w_b+w_s)}{\partial x^2}\\
&+\frac{\partial^2(w_b+w_s)}{\partial y^2}]-k_w[(w_b+w_s)\\
&-\mu\left(\frac{\partial^2(w_b+w_s)}{\partial x^2}+\frac{\partial^2(w_b+w_s)}{\partial y^2}\right)]=0
\end{aligned}
\tag{27}
$$

$$
\begin{aligned}
&-D_{11}^s\left[\frac{\partial^4 w_b}{\partial x^4}-\lambda\left(\frac{\partial^6 w_b}{\partial x^6}+\frac{\partial^6 w_b}{\partial x^4\partial y^2}\right)\right]\\
&+A_{55}^s\left[\frac{\partial^2 w_s}{\partial x^2}-\lambda\left(\frac{\partial^4 w_s}{\partial x^4}+\frac{\partial^4 w_s}{\partial x^2\partial y^2}\right)\right]\\
&+A_{44}^s\left[\frac{\partial^2 w_s}{\partial y^2}-\lambda\left(\frac{\partial^4 w_s}{\partial y^4}+\frac{\partial^4 w_s}{\partial y^2\partial x^2}\right)\right]\\
&-2(D_{12}^s+2D_{66}^s)\left[\frac{\partial^4 w_b}{\partial x^2\partial y^2}-\lambda\left(\frac{\partial^6 w_b}{\partial x^4\partial y^2}+\frac{\partial^6 w_b}{\partial x^2\partial y^4}\right)\right]\\
&-D_{22}^s\left[\frac{\partial^4 w_b}{\partial y^4}-\lambda\left(\frac{\partial^6 w_b}{\partial y^6}+\frac{\partial^6 w_b}{\partial y^4\partial x^2}\right)\right]\\
&-H_{11}^s\left[\frac{\partial^4 w_s}{\partial x^4}-\lambda\left(\frac{\partial^6 w_s}{\partial x^6}+\frac{\partial^6 w_s}{\partial x^4\partial y^2}\right)\right]\\
&-2(H_{12}^s+2H_{66}^s)\left[\frac{\partial^4 w_s}{\partial x^2\partial y^2}-\lambda\left(\frac{\partial^6 w_s}{\partial x^4\partial y^2}+\frac{\partial^6 w_s}{\partial x^2\partial y^4}\right)\right]\\
&-H_{22}^s\left[\frac{\partial^4 w_s}{\partial y^4}-\lambda\left(\frac{\partial^6 w_s}{\partial y^6}+\frac{\partial^6 w_s}{\partial y^4\partial x^2}\right)\right]\\
&-I_0\left[\frac{\partial^2(w_b+w_s)}{\partial t^2}-\mu\left(\frac{\partial^4(w_b+w_s)}{\partial t^2\partial x^2}+\frac{\partial^4(w_b+w_s)}{\partial t^2\partial y^2}\right)\right]\\
&+J_2[\frac{\partial^4 w_b}{\partial x^2\partial t^2}+\frac{\partial^4 w_b}{\partial y^2\partial t^2}-\mu(\frac{\partial^6 w_b}{\partial t^2\partial x^4}\\
&+2\frac{\partial^6 w_b}{\partial t^2\partial x^2\partial y^2}+\frac{\partial^6 w_b}{\partial t^2\partial y^4})]+K_2[\frac{\partial^4 w_s}{\partial x^2\partial t^2}+\frac{\partial^4 w_s}{\partial y^2\partial t^2}\\
&-\mu(\frac{\partial^6 w_s}{\partial t^2\partial x^4}+2\frac{\partial^6 w_s}{\partial t^2\partial x^2\partial y^2}+\frac{\partial^6 w_s}{\partial t^2\partial y^4})]\\
&-N_x^0(y)\left[1-\mu\left(\frac{\partial^2}{\partial x^2}+\frac{\partial^2}{\partial y^2}\right)\right]\frac{\partial^2(w_b+w_s)}{\partial x^2}-N_y^0(x)\\
&\left[1-\mu\left(\frac{\partial^2}{\partial x^2}+\frac{\partial^2}{\partial y^2}\right)\right]\frac{\partial^2(w_b+w_s)}{\partial y^2}\\
&+k_p\left[1-\mu\left(\frac{\partial^2}{\partial x^2}+\frac{\partial^2}{\partial y^2}\right)\right]\\
&\left[\frac{\partial^2(w_b+w_s)}{\partial x^2}+\frac{\partial^2(w_b+w_s)}{\partial y^2}\right]\\
&-k_w\left[(w_b+w_s)-\mu\left(\frac{\partial^2(w_b+w_s)}{\partial x^2}+\frac{\partial^2(w_b+w_s)}{\partial y^2}\right)\right]\\
&=0
\end{aligned}
\tag{28}
$$

3. Solution by Galerkin's method

One of the numerical approaches to investigate behavior of graphene sheets is to use Gelarkin's technique. Galerkin's Technique has been employed with the purpose of resolving the fundamental expressions of nonlocal strain gradient graphene thin sheets. Therefore, the displacement field is able to be solved through

$$w_b=\sum_{m=1}^{\infty}\sum_{n=1}^{\infty}W_{bmn}\Phi_{bm}(x)\,\Psi_{bn}(y)e^{i\omega_n t} \tag{29}$$

$$w_s=\sum_{m=1}^{\infty}\sum_{n=1}^{\infty}W_{smn}\Phi_{sm}(x)\,\Psi_{sn}(y)e^{i\omega_n t} \tag{30}$$

In the above equations (W_{bmn}, W_{smn}) represents the untold coefficients along with the functions viz., Φ_m & Ψ_n are satisfy the boundary conditions.

Boundary conditions must rely on and consider thin plate model that are essentially given as

$$
\begin{aligned}
&w_b=w_s=0,\\
&\frac{\partial^2 w_b}{\partial x^2}=\frac{\partial^2 w_s}{\partial x^2}=\frac{\partial^2 w_b}{\partial y^2}=\frac{\partial^2 w_s}{\partial y^2}=0\\
&\text{simply-supported edge}
\end{aligned}
\tag{31}
$$

$$
\begin{aligned}
&w_b=w_s=0,\\
&\frac{\partial w_b}{\partial x}=\frac{\partial w_s}{\partial x}=\frac{\partial w_b}{\partial y}=\frac{\partial w_s}{\partial y}=0\\
&\text{clamped edge}
\end{aligned}
\tag{32}
$$

Introducing the Eqs. (29)-(30) in Eqs. (27)-(28) and multiplying all the obtained expressions with $\Phi_{im}\Psi_{in}$ $(i=b,s)$ and then integrate the equations, which results in achieveing the expressions shown below.

$$
\begin{aligned}
&\int_0^b\int_0^a\Phi_{bm}\Psi_{bn}[-D_{11}[\frac{\partial^4\Phi_{bm}}{\partial x^4}\Psi_{bn}\\
&-\lambda(\frac{\partial^6\Phi_{bm}}{\partial x^6}\Psi_{bn}+\frac{\partial^4\Phi_{bm}}{\partial x^4}\frac{\partial^2\Psi_{bn}}{\partial y^2})]\\
&-2(D_{12}+2D_{66})[\frac{\partial^2\Phi_{bm}}{\partial x^2}\frac{\partial^2\Psi_{bn}}{\partial y^2}-\lambda(\frac{\partial^4\Phi_{bm}}{\partial x^4}\frac{\partial^2\Psi_{bn}}{\partial y^2}\\
&+\frac{\partial^2\Phi_{bm}}{\partial x^2}\frac{\partial^4\Psi_{bn}}{\partial y^4})]-D_{22}[\frac{\partial^4\Psi_{bm}}{\partial y^4}\Phi_{bn}\\
&-\lambda(\frac{\partial^6\Psi_{bm}}{\partial y^6}\Phi_{bn}+\frac{\partial^2\Phi_{bm}}{\partial x^2}\frac{\partial^4\Psi_{bn}}{\partial y^4})]\\
&-D_{11}^s\left[\frac{\partial^4\Phi_{sm}}{\partial x^4}\Psi_{sn}-\lambda\left(\frac{\partial^6\Phi_{sm}}{\partial x^6}\Psi_{sn}+\frac{\partial^4\Phi_{sm}}{\partial x^4}\frac{\partial^2\Psi_{sn}}{\partial y^2}\right)\right]\\
&-2(D_{12}^s+2D_{66}^s)[\frac{\partial^2\Phi_{sm}}{\partial x^2}\frac{\partial^2\Psi_{sn}}{\partial y^2}-\lambda(\frac{\partial^4\Phi_{sm}}{\partial x^4}\frac{\partial^2\Psi_{sn}}{\partial y^2}
\end{aligned}
\tag{33}
$$

$$+\frac{\partial^2\Phi_{sm}}{\partial x^2}\frac{\partial^4\Psi_{sn}}{\partial y^4})]-D_{22}^s[\frac{\partial^4\Psi_{sm}}{\partial y^4}\Phi_{sn}$$
$$-\lambda(\frac{\partial^6\Psi_{sm}}{\partial y^6}\Phi_{sn}+\frac{\partial^2\Phi_{sm}}{\partial x^2}\frac{\partial^4\Psi_{sn}}{\partial y^4})]$$
$$+I_0\omega^2[(\Phi_{bm}\Psi_{bn}+\Phi_{sm}\Psi_{sn})$$
$$-\mu(\frac{\partial^2\Phi_{bm}}{\partial x^2}\Psi_{bn}+\frac{\partial^2\Phi_{sm}}{\partial x^2}\Psi_{sn}+\frac{\partial^2\Psi_{sm}}{\partial y^2}\Phi_{sn}$$
$$+\frac{\partial^2\Psi_{bm}}{\partial y^2}\Phi_{bn})]-I_2\omega^2[\frac{\partial^2\Phi_{bm}}{\partial x^2}\Psi_{bn}+\frac{\partial^2\Psi_{bm}}{\partial y^2}\Phi_{bn}$$
$$-\mu(\frac{\partial^4\Phi_{bm}}{\partial x^4}\Psi_{bn}+2\frac{\partial^2\Phi_{bm}}{\partial x^2}\frac{\partial^2\Psi_{bn}}{\partial y^2}+\frac{\partial^b\Psi_{sm}}{\partial y^4}\Phi_{bn})]$$
$$-J_2\omega^2[\frac{\partial^2\Phi_{sm}}{\partial x^2}\Psi_{sn}+\frac{\partial^2\Psi_{sm}}{\partial y^2}\Phi_{sn}-\mu(\frac{\partial^4\Phi_{sm}}{\partial x^4}\Psi_{sn}$$
$$+2\frac{\partial^2\Phi_{sm}}{\partial x^2}\frac{\partial^2\Psi_{sn}}{\partial y^2}+\frac{\partial^4\Psi_{sm}}{\partial y^4}\Phi_{sn})]$$
$$-N_x^0(y)\left[1-\mu\left(\frac{\partial^2}{\partial x^2}+\frac{\partial^2}{\partial y^2}\right)\right]$$
$$\left[\frac{\partial^2\Phi_{bm}}{\partial x^2}\Psi_{bn}+\frac{\partial^2\Phi_{sm}}{\partial x^2}\Psi_{sn}\right]$$
$$-N_y^0(x)\left[1-\mu\left(\frac{\partial^2}{\partial x^2}+\frac{\partial^2}{\partial y^2}\right)\right]$$
$$\left[\frac{\partial^2\Psi_{sm}}{\partial y^2}\Phi_{sn}+\frac{\partial^2\Psi_{bm}}{\partial y^2}\Phi_{bn}\right]$$
$$+k_p(1-\mu(\frac{\partial}{\partial x^2}+\frac{\partial}{\partial x^2}))[(\frac{\partial^2\Phi_{bm}}{\partial x^2}\Psi_{bn}+\frac{\partial^2\Phi_{sm}}{\partial x^2}\Psi_{sn}$$
$$+\frac{\partial^2\Psi_{sm}}{\partial y^2}\Phi_{sn}+\frac{\partial^2\Psi_{bm}}{\partial y^2}\Phi_{bn})]$$
$$-k_w(1-\mu(\frac{\partial}{\partial x^2}+\frac{\partial}{\partial x^2}))(\Phi_{bm}\Psi_{bn}+\Phi_{sm}\Psi_{sn})]dxdy$$
$$=0 \tag{33}$$

$$\int_0^b\int_0^a\Phi_{sm}\Psi_{sn}[-D_{11}^s[\frac{\partial^4\Phi_{bm}}{\partial x^4}\Psi_{bn}$$
$$-\lambda(\frac{\partial^6\Phi_{bm}}{\partial x^6}\Psi_{bn}+\frac{\partial^4\Phi_{bm}}{\partial x^4}\frac{\partial^2\Psi_{bn}}{\partial y^2})]$$
$$-2(D_{12}^s+2D_{66}^s)[\frac{\partial^2\Phi_{bm}}{\partial x^2}\frac{\partial^2\Psi_{bn}}{\partial y^2}-\lambda(\frac{\partial^4\Phi_{bm}}{\partial x^4}\frac{\partial^2\Psi_{bn}}{\partial y^2}$$
$$+\frac{\partial^2\Phi_{bm}}{\partial x^2}\frac{\partial^4\Psi_{bn}}{\partial y^4})]-D_{22}^s[\frac{\partial^4\Psi_{bm}}{\partial y^4}\Phi_{bn}-\lambda(\frac{\partial^6\Psi_{bm}}{\partial y^6}\Phi_{bn}$$
$$+\frac{\partial^2\Phi_{bm}}{\partial x^2}\frac{\partial^4\Psi_{bn}}{\partial y^4})]-H_{11}^s[\frac{\partial^4\Phi_{sm}}{\partial x^4}\Psi_{sn}$$
$$-\lambda(\frac{\partial^6\Phi_{sm}}{\partial x^6}\Psi_{sn}+\frac{\partial^4\Phi_{sm}}{\partial x^4}\frac{\partial^2\Psi_{sn}}{\partial y^2})]$$
$$-2(H_{12}^s+2H_{66}^s)[\frac{\partial^2\Phi_{sm}}{\partial x^2}\frac{\partial^2\Psi_{sn}}{\partial y^2}-\lambda(\frac{\partial^4\Phi_{sm}}{\partial x^4}\frac{\partial^2\Psi_{sn}}{\partial y^2}$$
$$+\frac{\partial^2\Phi_{sm}}{\partial x^2}\frac{\partial^4\Psi_{sn}}{\partial y^4})]-H_{22}^s[\frac{\partial^4\Psi_{sm}}{\partial y^4}\Phi_{sn}-\lambda(\frac{\partial^6\Psi_{sm}}{\partial y^6}\Phi_{sn}$$
$$+\frac{\partial^2\Phi_{sm}}{\partial x^2}\frac{\partial^4\Psi_{sn}}{\partial y^4})]+I_0\omega^2[\Phi_{bm}\Psi_{bn}-\mu(\frac{\partial^2\Phi_{bm}}{\partial x^2}\Psi_{bn}$$
$$+\frac{\partial^2\Phi_{sm}}{\partial x^2}\Psi_{sn}+\frac{\partial^2\Psi_{sm}}{\partial y^2}\Phi_{sn}+\frac{\partial^2\Psi_{bm}}{\partial y^2}\Phi_{bn})]$$
$$-J_2\omega^2[\frac{\partial^2\Phi_{bm}}{\partial x^2}\Psi_{bn}+\frac{\partial^2\Psi_{bm}}{\partial y^2}\Phi_{bn}-\mu(\frac{\partial^4\Phi_{bm}}{\partial x^4}\Psi_{bn}$$
$$+2\frac{\partial^2\Phi_{bm}}{\partial x^2}\frac{\partial^2\Psi_{bn}}{\partial y^2}+\frac{\partial^b\Psi_{sm}}{\partial y^4}\Phi_{bn})]-K_2\omega^2[\frac{\partial^2\Phi_{sm}}{\partial x^2}\Psi_{sn}$$
$$+\frac{\partial^2\Psi_{sm}}{\partial y^2}\Phi_{sn}-\mu(\frac{\partial^4\Phi_{sm}}{\partial x^4}\Psi_{sn}+2\frac{\partial^2\Phi_{sm}}{\partial x^2}\frac{\partial^2\Psi_{sn}}{\partial y^2}$$
$$+\frac{\partial^4\Psi_{sm}}{\partial y^4}\Phi_{sn})]-N_x^0(y)\left[1-\mu\left(\frac{\partial^2}{\partial x^2}+\frac{\partial^2}{\partial y^2}\right)\right]$$
$$\left[\frac{\partial^2\Phi_{bm}}{\partial x^2}\Psi_{bn}+\frac{\partial^2\Phi_{sm}}{\partial x^2}\Psi_{sn}\right]$$
$$-N_y^0(x)\left[1-\mu\left(\frac{\partial^2}{\partial x^2}+\frac{\partial^2}{\partial y^2}\right)\right]$$
$$[\frac{\partial^2\Psi_{sm}}{\partial y^2}\Phi_{sn}+\frac{\partial^2\Psi_{bm}}{\partial y^2}\Phi_{bn}]+A_{55}^s[\frac{\partial^2\Phi_{sm}}{\partial x^2}\Psi_{sn}$$
$$-\lambda(\frac{\partial^4\Phi_{sm}}{\partial x^4}\Psi_{sn}+\frac{\partial^2\Phi_{sm}}{\partial x^2}\frac{\partial^2\Psi_{sn}}{\partial y^2})]$$
$$+A_{44}^s[\frac{\partial^2\Psi_{sm}}{\partial y^2}\Phi_{sn}-\lambda(\frac{\partial^4\Psi_{sm}}{\partial y^4}\Phi_{sn}+\frac{\partial^2\Phi_{sm}}{\partial x^2}\frac{\partial^2\Psi_{sn}}{\partial y^2})$$
$$+k_p(1-\mu(\frac{\partial}{\partial x^2}+\frac{\partial}{\partial x^2}))[\frac{\partial^2\Phi_{bm}}{\partial x^2}\Psi_{bn}+\frac{\partial^2\Phi_{sm}}{\partial x^2}\Psi_{sn}$$
$$+\frac{\partial^2\Psi_{sm}}{\partial y^2}\Phi_{sn}+\frac{\partial^2\Psi_{bm}}{\partial y^2}\Phi_{bn})]$$
$$-k_w(1-\mu(\frac{\partial}{\partial x^2}+\frac{\partial}{\partial x^2}))(\Phi_{bm}\Psi_{bn}+\Phi_{sm}\Psi_{sn})]dxdy$$
$$=0 \tag{34}$$

The function Φ_m is for variying boundary conditions and happens to be given as

$$\text{SS:}\quad \begin{matrix}\Phi_m(x)=\sin(\lambda_m x)\\ \lambda_m=\dfrac{m\pi}{a}\end{matrix} \tag{35}$$

$$\text{CC:}\quad \begin{matrix}\Phi_m(x)=\sin(\lambda_m x)-\sinh(\lambda_m x)\\ \qquad -\xi_m(\cos(\lambda_m x)-\cosh(\lambda_m x))\\ \xi_m=\dfrac{\sin(\lambda_m x)-\sinh(\lambda_m x)}{\cos(\lambda_m x)-\cosh(\lambda_m x)}\\ \lambda_1=4.730,\quad \lambda_2=7.853,\quad \lambda_3=10.996,\\ \lambda_4=14.137,\quad \lambda_{m\geq 5}=\dfrac{(m+0.5)\pi}{a}\end{matrix} \tag{36}$$

$$\text{CS:}\quad \begin{matrix}\Phi_m(x)=\sin(\lambda_m x)-\sinh(\lambda_m x)\\ \qquad -\xi_m(\cos(\lambda_m x)-\cosh(\lambda_m x))\\ \xi_m=\dfrac{\sin(\lambda_m x)+\sinh(\lambda_m x)}{\cos(\lambda_m x)+\cosh(\lambda_m x)}\\ \lambda_1=3.927,\quad \lambda_2=7.069,\quad \lambda_3=10.210,\\ \lambda_4=13.352,\quad \lambda_{m\geq 5}=\dfrac{(m+0.25)\pi}{a}\end{matrix} \tag{37}$$

Now, in order to achieve the new function Ψ_n, *x*, *m* & *a* by *y*, *n* & *b* must be replaced respectively. Afterwards, the coefficient matrix of all the aforementioned expressions above gives the eigenvalue problem

$$([K]+\omega^2[M])\begin{Bmatrix}W_b\\W_s\end{Bmatrix}=0 \tag{38}$$

Here, [M] & [K] represents the mass and stiffness matrix correspondingly. Now to compute the problem further, putting the coefficient matrix equals to zero

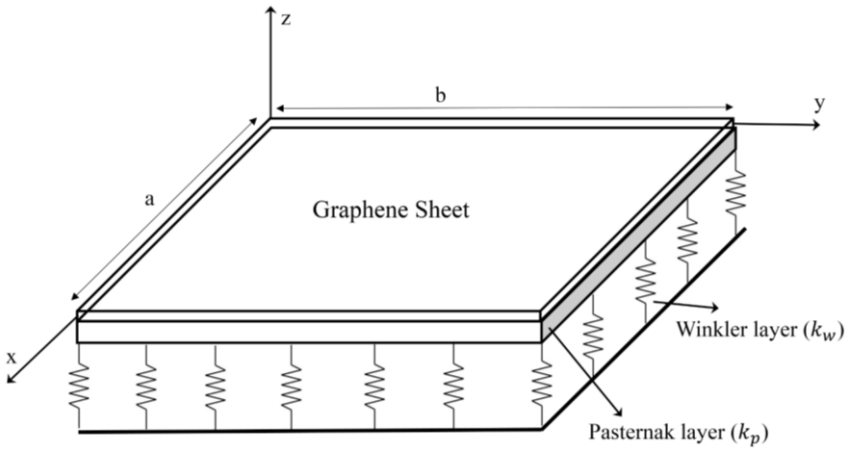

Fig. 1 The configuration of graphene sheet resting on elastic substrate

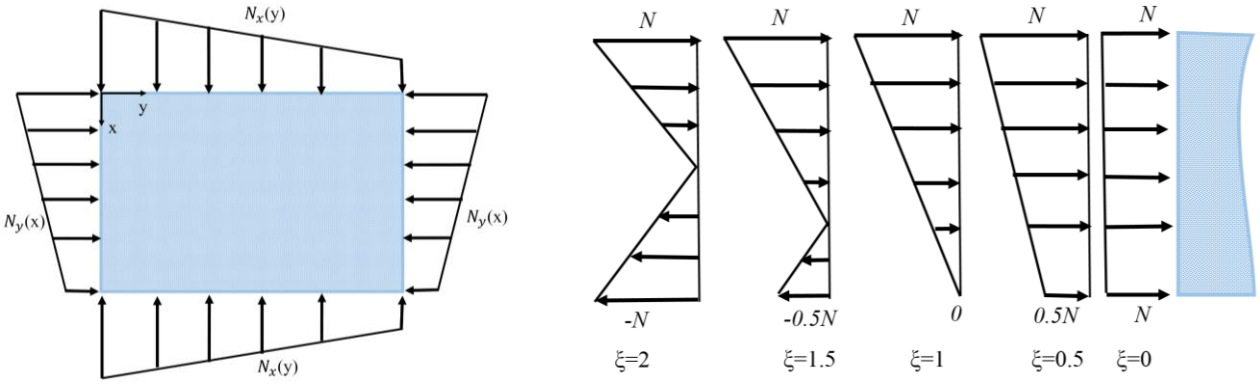

Fig. 2 Various cases of in-plane bending loads

(necessary and sufficient condition) which gives the natural frequencies.

Note: calculations are executed by including the dimensionless expressions shown below as

$$\hat{\omega} = \omega \frac{a^2}{h}\sqrt{\frac{\rho}{E}}, \qquad K_w = k_w \frac{a^4}{D^*}, \qquad K_p = k_p \frac{a^2}{D^*}, \qquad D^* = \frac{Eh^3}{12(1-v^2)}, \quad \bar{N} = N\frac{a^2}{D^*} \tag{39}$$

4. Numerical results and discussions

Following the two-variable shear deformation concept, this is section is going to delineate the vibration characteristics of thin graphene sheets are resting over an elastic material half-space subjected to face in-plane loading. The considered structure studies the more precise examination of graphene sheets form the two-scale coefficients are in connection with the strain gradient and nonlocal effects. Graphene thin sheets have the following material properties: E = 1 TPa, v = 0.19, ρ = 2300 kg/m^3 and graphene sheet is 0.34 nm thick. Figs. 1 and 2, represents the schematics of graphene sheets having in-plane loading. Futhermore, validation of natural frequencies of thin graphene sheets is followed by Sobhy (2014) for the distinct

Table 1 A comparison of the natural frequency of a graphene sheet for various nonlocal and foundation parameters (a/h = 10)

μ	K_w = 0, K_p = 0		K_w = 100, K_p = 0		K_w = 0, K_p = 20	
	Sobhy (2014)	Present	Sobhy (2014)	Present	Sobhy (2014)	Present
0	1.93861	1.93861	2.18396	2.18396	2.7841	2.78410
1	1.17816	1.17816	1.54903	1.54903	2.31969	2.31969
2	0.92261	0.92261	1.36479	1.36479	2.20092	2.20092
3	0.78347	0.78347	1.27485	1.27485	2.14629	2.14629
4	0.69279	0.69279	1.22122	1.22122	2.11486	2.11486

nonlocal parameters (μ = 0, 1, 2, 3, 4 nm^2) & foundation constants ({K_w, K_p} = {(0,0), (100,0), (0,20)} along with also achieved frequency by Galerkin technique is in well agreement with Sobhy (2014), which is presented in Table 1. Length scale parameter or the strain gradient is set to zero (λ = 0) for comparison study.

Further into discussion, analysis of strain gradient and nonlocal influence on vibrational frequencies of thin sheets of graphene materials against non-dimensionless load is delineated in Fig. 3 for a/h = 10. When λ = 0, graphene sheets natural frequencies are achieved following the

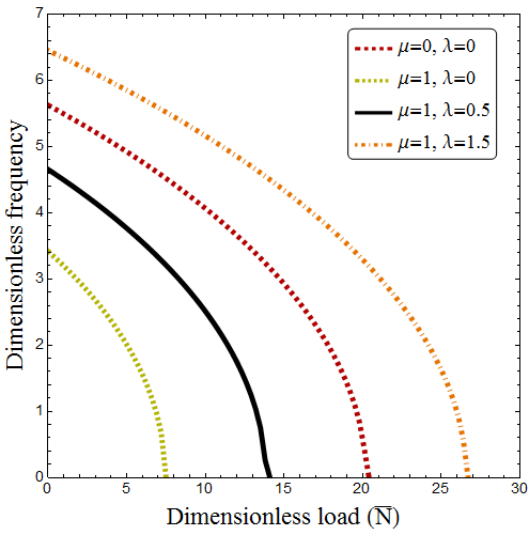

Fig. 3 Variation of dimensionless frequency versus dimensionless load for different nonlocal and strain gradient parameters (a/h = 10, ξ = 0.5)

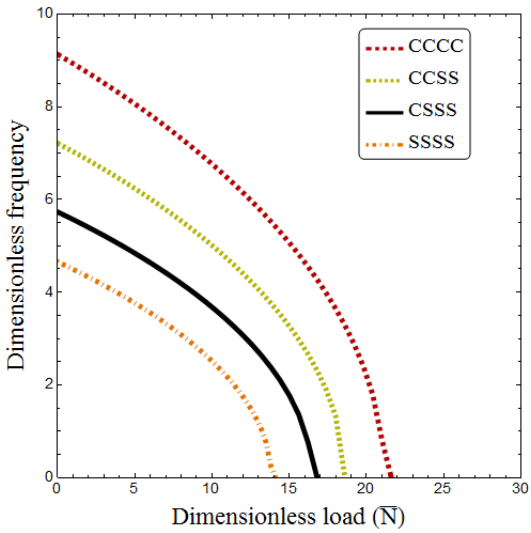

Fig. 5 Variation of dimensionless frequency versus dimensionless load for different boundary conditions (a/h = 10, ξ = 0.5, μ = 1 nm^2, λ = 0.5 nm^2)

elasticity theory. When both μ = 0 & λ = 0, the figures render significant outcomes following original continuum mechanics. When the in-plane load value is fixed, it is recorded that graphene thin sheet natural frequency decreases with the increment in the value of nonlocal parameter. The results delineate how the nonlocal parameter develops an influence of stiffness-softening which shows there is in fact a decrease with the value of natural frequency. Another factor discovered is the influence the nonlocal parameter has on frequency (natural) mainly relying on the length scale or even the strain gradient parameter. As outcomes, stiffness-hardening influence is because of the strain gradients due to graphene sheet natural frequency grows in value with increments in the value of length scale parameter. Furthermore, it is observed that the increment in the non-dimensional load reduces the material plate natural and stiffness upto the critical point i.e., when the frequency of the considered structure becomes zero. On the achieved critical point, the thin graphene sheets only buckle and do not follow the oscillations. So, there is a dependency of achieved critical points over length scale parameter. Therefore, in nonlocal strain gradient theory, when we use the concept of length scale parameter, gives the high value of critical point unless which is not achieved by using the nonlocal theory. Therefore, the result indicate that, it is significant to take both length scale along with nonlocal parameters in examination of thin graphene material sheets.

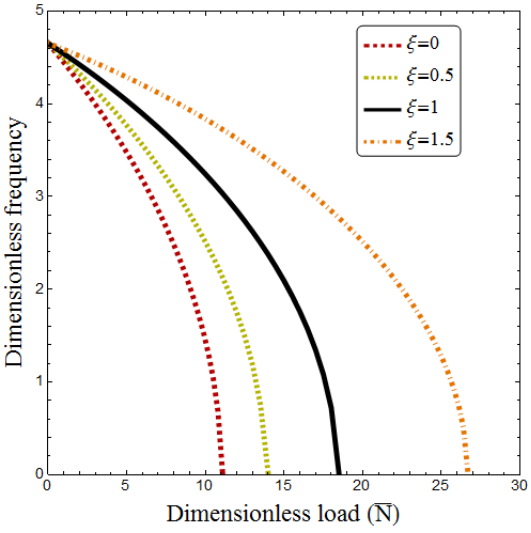

Fig. 4 Variation of dimensionless frequency versus dimensionless load for different load factors (a/h = 10, μ = 1 nm^2, λ = 0.5 nm^2)

Additionally, Fig. 4 delineate the non-dimensional frequency variation of thin graphene material sheets of nonlocal strain against non-dimensionless load for varied load factors, when there is a fixed value of a/h = 10, μ = 1 nm^2 and λ = 0.5 nm^2. In-plane loading decreases the stiffness of the plate and the influences remarkably on the structure performance. So, it is noticeable that, as if there is an increment in the load factor which leads to the increment in the non-dimensional frequencies. As a result, critical load buckling shifted to the right side of the framework because of increment of the load factor, the in-plane load reduces.

Now, Fig. 5 depicts the non-dimensional frequency variation of the considered nonlocal strain gradient graphene against the non-dimensional load for distinct boundary condition at a/h = 10, ξ = 0.5, μ = 1 nm^2 and λ = 0.5 nm^2. As we increase the total amount of clamped edges to make the graphene sheets more rigid, which results for increment in the natural frequency. As outcomes, achieved critical buckling loads of the considered structure of different boundary conditions follows the order: CCCC > CCSS > CSSS > SSSS.

Moving on, Fig. 6 signifies the influence that the Winkler-Pasternak foundation has on nonlocal strain gradient thin graphene material sheets vibrational frequencies at points a/h = 10, ξ = 0.5, μ = 1 nm^2, λ = 0.5 nm^2. From the figure, it is observed how the graphene

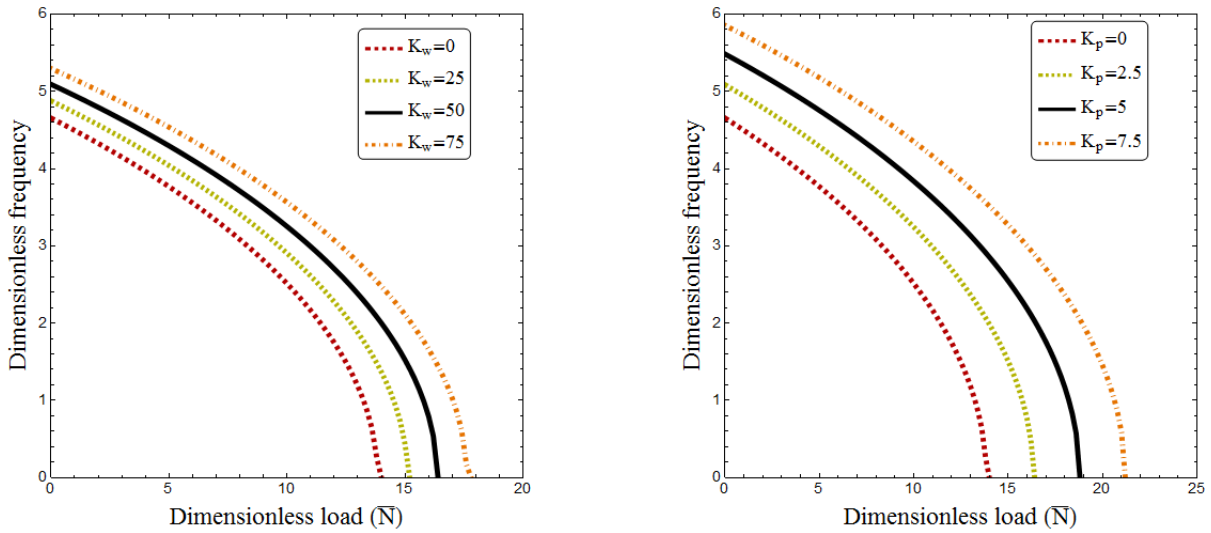

Fig. 6 Variation of dimensionless frequency versus dimensionless load for different Winkler and Pasternak parameters (a/h = 10, ξ = 0.5, μ = 1 nm^2, λ = 0.5 nm^2)

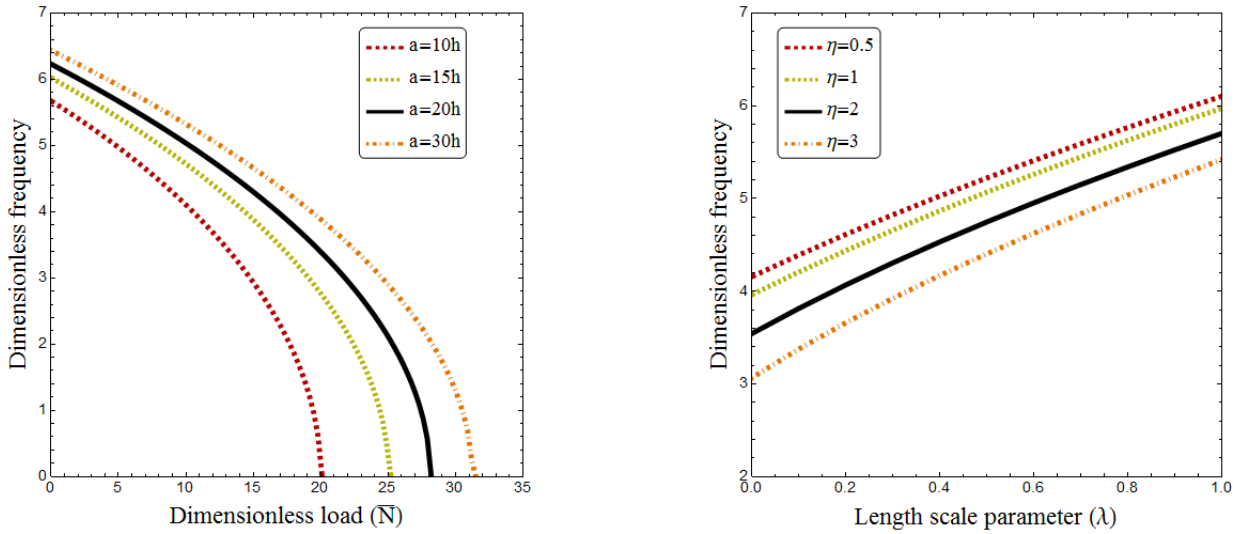

Fig. 7 Variation of dimensionless frequency versus dimensionless load for different values of plate length (ξ = 0.5, $\eta = 1$, K_w = 25, K_p = 5, μ = 1 nm^2, λ = 0.5 nm^2)

Fig. 8 Variation of dimensionless frequency versus length scale parameter for different values of load factor (ξ = 0.5, N = 5, K_w = 25, K_p = 5, μ = 1 nm^2)

material sheet vibration behavior relies tremendoudly on both the Pasternak as well as the Winkler parameters. Hence, Pasternak thin film and Winkler thin layer creates a continuous and discontinuous interaction with graphene material sheet. The bending rigidity of the considered material plates graphene has been enhanced by increasing the value of Pasternak and Winkler parameters. Moreover, Pasternak thin film influences more on natural frequency in comparison to Winkler thin film. It is noticeable that increment in the foundation variables produces higher critical buckling loads.

Subsequentally, Fig. 7 reveals the non-dimensional frequency variation against non-dimensionl in-plane bending load in consideration of various side-to-thickness ratios (a/h) at ξ = 0.5, $\eta = 1$, K_w = 25, K_p = 5, μ = 1 nm^2, λ = 0.5 nm^2. From the Fig. 7 it can be observed that graphene material thin sheets by changing more side-to-thickness ratios creates frequency that is more vibrational means have high critical buckling load.

Influence of load factors ($\eta = N_y/N_x$) & ξ is shown in Figs. 8 and 9 on non-dimensional frequency variation of graphene material thin sheets against length scale parameter respectively when N = 5, K_w = 25, K_p = 5, μ = 1 nm^2. If there is an increment in the measure of biaxial load factor (η) which leads to the influence of applied load and i.e., more significant in y direction. However, which leads to a remarkable decrement in the graphene plate natural frequencies and stiffness. Moreover, with the increment in the in-plane bending load factor (ξ), the outcome of the load applied gets in the decrement and as a result, there is a significant increment in vibration frequencies. Here ξ = 2,

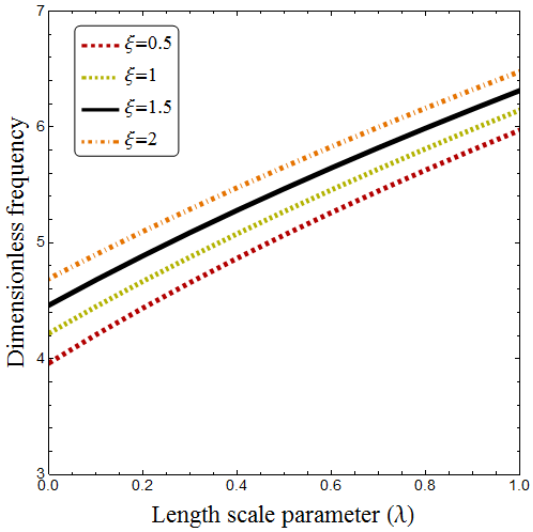

Fig. 9 Variation of dimensionless frequency versus length scale parameter for different values of load factor ($\eta = 1$, N = 5, K_w = 25, K_p = 5, μ = 1 nm^2)

the graphene material thin sheet is having pure bending and it has the highest frequency in comparison with other bending loads.

5. Conclusions

The current original research paper carries what is known as the nonlocal strain gradient theory which makes use of potentially scrutinizing the free quivering nature of single-layer graphene folio or sheets under in-plane bending loads placed on the elastic mediums that consequently apply an advanced two-variable plate theory. What the theory does is it generally presents the two scale variables formally, in relation with the strain gradient along with nonlocal influences in order to apprehend stiffness-hardening & softening effect. Moreover, Hamilton's principle is studied and integrated with the aim to achieve the fundamental basic equation in regard to the considered study i.e., nonlocal strain gradient graphene folio theory. A Galerkin's technique has been applied with the intent of solving the fundamental equations for the distinct boundary conditions. Influence of the distinct factors which can be in-plane loading, length scale parameter, load factor, elastic foundation, boundary conditions, and nonlocal parameter on vibration properties of graphene sheets are investigated. Pasternak thin film influences more on natural frequency in comparison to Winkler thin film. It is noticed that increment in the foundation parameters produces higher critical buckling loads. From study, there are some remarkable outcomes:

- The temperature increment deploys the thin plate natural frequencies and stiffness results into the degradation up to a certain critical point whenever the resultant frequencies approaches to the zero value.
- It is noticeable that increment in the foundation parameters produces higher critical buckling loads.
- In nonlocal strain gradient theory this present research uses the concept of length scale parameter, gives the high value of critical point unless which is not achieve by using the nonlocal theory.
- Achieved critical buckling loads of the considered structure of different boundary condition follows the order: CCCC > CCSS > CSSS > SSSS.
- Although, it is clear from the achieved results: nonlocal strain gradient theory obtained higher critical buckling loads in respect to the nonlocal elasticity theory.
- The natural frequency gets increment along with the increment in the length scale parameter, results into the stiffness-hardening influence because of strain gradients.
- In the increment of in-plane bending load factor, then there is a drop in the value of applied load resultant and which leads in the increment of the value of vibration frequencies.
- Absolutely, in view of strain gradient influences to deferment in the buckling of graphene material folio.

References

Aksencer, T. and Aydogdu, M. (2011), "Levy type solution method for vibration and buckling of nanoplates using nonlocal elasticity theory", *Physica E*: *Low-dimens*. *Syst*. *Nanostruct*., **43**(4), 954-959. https://doi.org/10.1016/j.physe.2010.11.024

Ansari, R. and Sahmani, S. (2013), "Prediction of biaxial buckling behavior of single-layered graphene sheets based on nonlocal plate models and molecular dynamics simulations", *Appl*. *Mathe*. *Model*., **37**(12), 7338-7351. https://doi.org/10.1016/j.apm.2013.03.004

Ansari, R., Arash, B. and Rouhi, H. (2011), "Vibration characteristics of embedded multi-layered graphene sheets with different boundary conditions via nonlocal elasticity", *Compos*. *Struct*., **93**(9), 2419-2429. https://doi.org/10.1016/j.compstruct.2011.04.006

Bessaim, A., Houari, M.S.A., Bernard, F. and Tounsi, A. (2015), "A nonlocal quasi-3D trigonometric plate model for free vibration behaviour of micro/nanoscale plates", *Struct*. *Eng*. *Mech*., *Int*. *J*., **56**(2), 223-240. https://doi.org/10.12989/sem.2015.56.2.223

Ebrahimi, F. and Barati, M.R. (2016a), "Magneto-electro-elastic buckling analysis of nonlocal curved nanobeams", *Eur*. *Phys*. *J*. *Plus*, **131**(9), 346. https://doi.org/10.1140/epjp/i2016-16346-5

Ebrahimi, F. and Barati, M.R. (2016b), "Static stability analysis of smart magneto-electro-elastic heterogeneous nanoplates embedded in an elastic medium based on a four-variable refined plate theory", *Smart Mater*. *Struct*., **25**(10), 105014. https://doi.org/10.1088/0964-1726/25/10/105014

Ebrahimi, F. and Barati, M.R. (2016c), "Temperature distribution effects on buckling behavior of smart heterogeneous nanosize plates based on nonlocal four-variable refined plate theory", *Int*. *J*. *Smart Nano Mater*., **7**(3), 119-143. https://doi.org/10.1080/19475411.2016.1223203

Ebrahimi, F. and Barati, M.R. (2016d), "An exact solution for buckling analysis of embedded piezo-electro-magnetically actuated nanoscale beams", *Adv*. *Nano Res*., *Int*. *J*., **4**(2), 65-84. https://doi.org/10.12989/anr.2016.4.2.065

Ebrahimi, F. and Barati, M.R. (2016e), "Buckling analysis of smart size-dependent higher order magneto-electro-thermo-elastic functionally graded nanosize beams", *J*. *Mech*., **33**(1), 23-33. https://doi.org/10.1017/jmech.2016.46

Ebrahimi, F. and Barati, M.R. (2016f), "Buckling analysis of nonlocal third-order shear deformable functionally graded piezoelectric nanobeams embedded in elastic medium", *J. Brazil. Soc. Mech. Sci. Eng.*, **39**, 937-952. https://doi.org/10.1007/s40430-016-0551-5

Ebrahimi, F. and Barati, M.R. (2016g), "Magnetic field effects on buckling behavior of smart size-dependent graded nanoscale beams", *Eur. Phys. J. Plus*, **131**(7), 238. https://doi.org/10.1140/epjp/i2016-16238-8

Ebrahimi, F. and Barati, M.R. (2016h), "Vibration analysis of nonlocal beams made of functionally graded material in thermal environment", *Eur. Phys. J. Plus*, **131**(8), 279. https://doi.org/10.1140/epjp/i2016-16279-y

Ebrahimi, F. and Barati, M.R. (2016i), "Vibration analysis of smart piezoelectrically actuated nanobeams subjected to magneto-electrical field in thermal environment", *J. Vib. Control*, **24**(3), 549-564. https://doi.org/10.1177/1077546316646239

Ebrahimi, F. and Barati, M.R. (2016j), "A nonlocal higher-order refined magneto-electro-viscoelastic beam model for dynamic analysis of smart nanostructures", *Int. J. Eng. Sci.*, **107**, 183-196. https://doi.org/10.1016/j.ijengsci.2016.08.001

Ebrahimi, F. and Barati, M.R. (2016k), "Small-scale effects on hygro-thermo-mechanical vibration of temperature-dependent nonhomogeneous nanoscale beams", *Mech. Adv. Mater. Struct.*, **24**(11), 924-936. https://doi.org/10.1080/15376494.2016.1196795

Ebrahimi, F. and Barati, M.R. (2016l), "A unified formulation for dynamic analysis of nonlocal heterogeneous nanobeams in hygro-thermal environment", *Appl. Phys. A*, **122**(9), 792. https://doi.org/10.1080/19475411.2016.1191556

Ebrahimi, F. and Barati, M.R. (2016m), "Electromechanical buckling behavior of smart piezoelectrically actuated higher-order size-dependent graded nanoscale beams in thermal environment", *Int. J. Smart Nano Mater.*, **7**(2), 69-90. https://doi.org/10.1080/19475411.2016.1191556

Ebrahimi, F. and Barati, M.R. (2016n), "Vibration analysis of nonlocal beams made of functionally graded material in thermal environment", *Eur. Phys. J. Plus*, **131**(8), 279. https://doi.org/10.1177/1077546316646239

Ebrahimi, F. and Barati, M.R. (2016o), "A unified formulation for dynamic analysis of nonlocal heterogeneous nanobeams in hygro-thermal environment", *Appl. Phys. A*, **122**(9), 792. https://doi.org/10.1007/s00339-016-0322-2

Ebrahimi, F. and Barati, M.R. (2016p), "A nonlocal higher-order refined magneto-electro-viscoelastic beam model for dynamic analysis of smart nanostructures", *Int. J. Eng. Sci.*, **107**, 183-196. https://doi.org/10.1016/j.ijengsci.2016.08.001

Ebrahimi, F. and Barati, M.R. (2016q), "Hygrothermal buckling analysis of magnetically actuated embedded higher order functionally graded nanoscale beams considering the neutral surface position", *J. Thermal Stress.*, **39**(10), 1210-1229. https://doi.org/10.1080/01495739.2016.1215726

Ebrahimi, F. and Barati, M.R. (2016r), "Vibration analysis of smart piezoelectrically actuated nanobeams subjected to magneto-electrical field in thermal environment", *J. Vib. Control*, **24**(3), 549-564. https://doi.org/10.1177/1077546316646239

Ebrahimi, F. and Barati, M.R. (2016s), "Static stability analysis of smart magneto-electro-elastic heterogeneous nanoplates embedded in an elastic medium based on a four-variable refined plate theory", *Smart Mater. Struct.*, **25**(10), 105014. https://doi.org/10.1088/0964-1726/25/10/105014

Ebrahimi, F. and Salari, E. (2015), "Thermo-mechanical vibration analysis of a single-walled carbon nanotube embedded in an elastic medium based on higher-order shear deformation beam theory", *J. Mech. Sci. Technol.*, **29**(9), 3797-3803. https://doi.org/10.1007/s12206-015-0826-2

Ebrahimi, F. and Shafiei, N. (2016), "Influence of initial shear stress on the vibration behavior of single-layered graphene sheets embedded in an elastic medium based on Reddy's higher-order shear deformation plate theory", *Mech. Adv. Mater. Struct.*, **24**(9), 761-772. https://doi.org/10.1080/15376494.2016.1196781

Eringen, A.C. (1983), "On differential equations of nonlocal elasticity and solutions of screw dislocation and surface waves", *J. Appl. Phys.*, **54**(9), 4703-4710. https://doi.org/10.1063/1.332803

Eringen, A.C. and Edelen, D.G.B. (1972), "On nonlocal elasticity", *Int. J. Eng. Sci.*, **10**(3), 233-248. https://doi.org/10.1016/0020-7225(72)90039-0

Farajpour, A., Shahidi, A.R., Mohammadi, M. and Mahzoon, M. (2012), "Buckling of orthotropic micro/nanoscale plates under linearly varying in-plane load via nonlocal continuum mechanics", *Compos. Struct.*, **94**(5), 1605-1615. https://doi.org/10.1016/j.compstruct.2011.12.032

Hashemi, S.H., Mehrabani, H. and Ahmadi-Savadkoohi, A. (2015), "Exact solution for free vibration of coupled double viscoelastic graphene sheets by viscoPasternak medium", *Compos. Part B: Eng.*, **78**, 377-383. https://doi.org/10.1016/j.compositesb.2015.04.008

Henderson, J.P., Plummer, A. and Johnston, N. (2018), "An electro-hydrostatic actuator for hybrid active-passive vibration isolation", *Int. J. Hydromechatron.*, **1**(1), 47-71. https://doi.org/10.1504/IJHM.2018.090305

Lam, D.C.C., Yang, F., Chong, A.C.M., Wang, J. and Tong, P. (2003), "Experiments and theory in strain gradient elasticity", *J. Mech. Phys. Solids*, **51**(8), 1477-1508. https://doi.org/10.1016/S0022-5096(03)00053-X

Mohammadi, M., Goodarzi, M., Ghayour, M. and Farajpour, A. (2013), "Influence of in-plane pre-load on the vibration frequency of circular graphene sheet via nonlocal continuum theory", *Compos. Part B: Eng.*, **51**, 121-129. https://doi.org/10.1016/j.compositesb.2013.02.044

Mohammadi, M., Farajpour, A., Moradi, A. and Ghayour, M. (2014), "Shear buckling of orthotropic rectangular graphene sheet embedded in an elastic medium in thermal environment", *Compos. Part B: Eng.*, **56**, 629-637. https://doi.org/10.1016/j.compositesb.2013.08.060

Murmu, T., McCarthy, M.A. and Adhikari, S. (2013), "In-plane magnetic field affected transverse vibration of embedded single-layer graphene sheets using equivalent nonlocal elasticity approach", *Compos. Struct.*, **96**, 57-63. https://doi.org/10.1016/j.compstruct.2012.09.005

Narendar, S. and Gopalakrishnan, S. (2012), "Scale effects on buckling analysis of orthotropic nanoplates based on nonlocal two-variable refined plate theory", *Acta Mechanica*, **223**(2), 395-413. https://doi.org/10.1007/s00707-011-0560-5

Pradhan, S.C. and Kumar, A. (2011), "Vibration analysis of orthotropic graphene sheets using nonlocal elasticity theory and differential quadrature method", *Compos. Struct.*, **93**(2), 774-779. https://doi.org/10.1016/j.compstruct.2010.08.004

Pradhan, S.C. and Murmu, T. (2009), "Small scale effect on the buckling of single-layered graphene sheets under biaxial compression via nonlocal continuum mechanics", *Computat. Mater. Sci.*, **47**(1), 268-274. https://doi.org/10.1016/j.commatsci.2009.08.001

Shen, Z.B., Tang, H.L., Li, D.K. and Tang, G.J. (2012), "Vibration of single-layered graphene sheet-based nanomechanical sensor via nonlocal Kirchhoff plate theory", *Computat. Mater. Sci.*, **61**, 200-205. https://doi.org/10.1016/j.commatsci.2012.04.003

Sobhy, M. (2014), "Thermomechanical bending and free vibration of single-layered graphene sheets embedded in an elastic medium", *Physica E: Low-dimens. Syst. Nanostruct.*, **56**, 400-409. https://doi.org/10.1016/j.physe.2013.10.017

Stelson, K.A. (2018), "Academic fluid power research in the USA", *Int. J. Hydromechatron.*, **1**(1), 126-152.

Tian, T., Nakano, M. and Li, W. (2018), "Applications of shear

thickening fluids: a review", *Int. J. Hydromechatron*., **1**(2), 238-257. https://doi.org/10.1504/IJHM.2018.092733

CC